

A UNIFIED APPROACH FOR THE ANALYSIS OF BRIDGES, PLATES AND AXISYMMETRIC SHELLS USING THE LINEAR MINDLIN STRIP ELEMENT

E. OÑATE and B. SUAREZ

E.T.S. Ingenieros de Caminos, Jorge Girona Salgado, 31, Barcelona, 34 Spain

(Received 29 April 1982; received for publication 3 August 1982)

Abstract—In this paper a finite strip formulation which allows to treat bridges, axisymmetric shells or plate structures of constant transverse cross section in an easily and unified manner is presented. The formulation is based on Mindlin's shell plate theory. One dimensional finite elements are used to discretize the transverse section and Fourier expansions are used to define the longitudinal/circumferential behavior of the structure. The element used is the simple two noded strip element with just one single integrating point. This allows to obtain all the element matrices in an explicit and economical form. Numerical examples for a variety of straight and curve bridges, axisymmetric shells and plate structures which show the efficiency of the formulation and accuracy of the linear strip element are given.

INTRODUCTION

It is well known that the analysis of structures which present constant material and geometrical properties along a particular direction, can be extremely simplified by the combined use of finite elements and Fourier expansions to model the transversal and longitudinal behaviour of the structure respectively. This procedure was first used in the context of plate bending analysis by Cheung[1,2], who named it "the finite strip method". Later Cheung[3-6], Loo and Cusens[7,8] amongst many others, extended the applications of the strip method to cover the analysis of folded plate and bridge structures[9]. The original "plate strip elements" developed by the referred authors were based on Kirchhoff's plate theory[1]. Therefore, the range of applicability of the method was restricted to structures composed of "thin" elements only.

Many reinforced and prestressed concrete bridges present components which can not clearly be classified as "thin" within the context of Kirchhoff's hypothesis and the use of this theory can produce inaccurate numerical results. This fact, together with the need of overcoming some of the problems which Kirchhoff's theory presents in the finite element context (i.e. the requirement of $C(1)$ continuity for the displacement variables)[9], has progressively encouraged many researchers to use Mindlin's plate theory[10] for the development of simpler and more accurate elements for the analysis of shell and plates. Mindlin's theory takes into account the effect of transverse shear deformation which it makes it valid for thick plate situations, requires only $C(0)$ continuity for the variables and it allows an independent interpolation of displacements and slopes. Benson and Hinton[11] extended this theory in the context of the finite strip method for the static and dynamic analysis of plates using the 3-noded strip element. Oñate[12] extended the same element to deal with straight box girder bridges.

Mindlin's plate and shell elements worked originally well for thick or moderately thin structures. However, some deficiencies were found when they were used to deal with very thin situations. These problems, nowadays

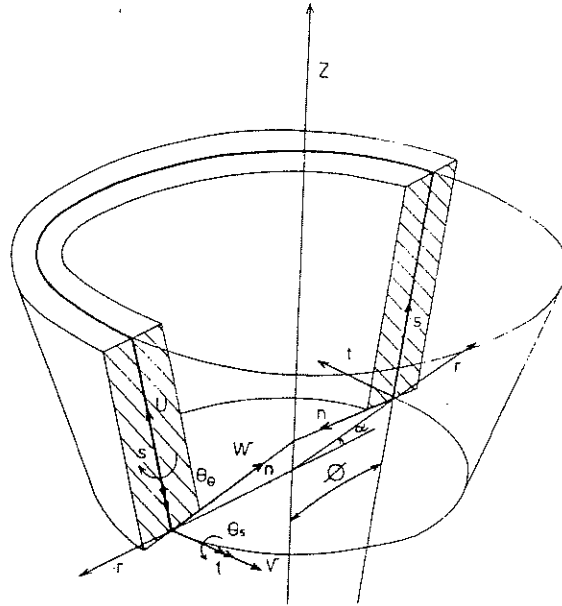
fully understood, are due to the numerical over stiffness effect (commonly known as "locking") induced in the stiffness matrix by the shear terms as the thickness of the plate reduces. The simplest artifice to overcome this problem seems to be the use of "reduced integration" techniques by which the parasitic effect of shear is eliminated via a subintegration of the terms of the stiffness matrix due to shear. Applications of these ideas have produced a wide range of new successful finite elements for the analysis of thick and thin plate and shell structures[13-16].

Suarez[17] and Oñate *et al.*[18] have recently studied the reduced integration family of Mindlin plate strip elements. They show how the linear strip element with just one single integrating point to evaluate all integrals is extremely simple and accurate for the static analysis of both thick and thin plates. The objective of this paper is to show how the linear strip element can be similarly used with success for both straight and curved bridges and axisymmetric shell analysis. The paper is structured in two parts. In the first, the general strip formulation to deal with curved and straight bridges and plates is presented. The second part of the paper deals with axisymmetric shell structures under arbitrary loading as a straightforward extension of the formulation presented in the first part.

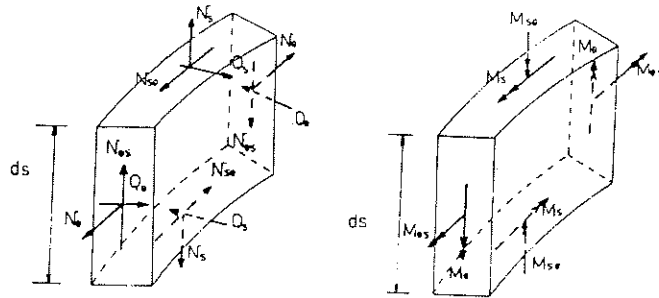
Special attention is focused in showing the analogy between the formulations for the different structural topologies and how the strip approach allows to treat them all in a simple and unified manner. Finally, numerical examples which show the adequacy of the formulation and the accuracy of the linear strip element for the static analysis of plates, bridges and axisymmetric shells are given.

BRIDGES AND PLATES

We will start from the most general case of a curved bridge with circular plant formed by tronconical shell elements like the one shown in Fig. 1. It will be shown how the formulation for straight bridges and plates can be considered as a particular case of the formulation presented here below.



1a Sign convention for displacements



1b Sign convention for resultant stresses

Fig. 1. Sign convention for displacements and resultant stresses in a troncoconical shell.

1.1 Curved bridges

Displacement field. Consider the tronconical shell element of Fig. 1. The three displacements of a generic point across the wall thickness can be easily expressed in terms of the three displacements and two rotations of the corresponding point in the middle surface as

$$\begin{aligned} u(s, \theta, n) &= u_0(s, \theta) + n\theta_s(s, \theta) \\ v(s, \theta, n) &= v_0(s, \theta) + n\theta_\theta(s, \theta) \\ w(s, \theta, n) &= w_0(s, \theta) \end{aligned} \quad (1)$$

where u_0, v_0 and w_0 are the displacements of a generic point of the shell middle surface and θ_s and θ_θ the rotations of the normal contained in the planes sn and tn respectively (see Fig. 1). In Mindlin-Reissner theory these rotations can be expressed as sum of the change in slope of the middle surface before and after deformation and an extra average rotation ϕ due to the effect of shear [10], i.e.

$$\begin{aligned} \theta_s &= -\frac{\partial w}{\partial s} + \phi_s \\ \theta_\theta &= -\frac{\partial w}{\partial \theta} + \phi_\theta \end{aligned} \quad (2)$$

Strain field. For the definition of strains we will adopt Washizu's tronconical shell theory [19] which defines the

relevant strains in the local system s, t, n (see Fig. 1) as

$$\bar{\epsilon} = \begin{Bmatrix} \epsilon_s \\ \epsilon_\theta \\ \gamma_{s\theta} \\ \gamma_{sn} \\ \gamma_{\theta n} \end{Bmatrix} = \begin{Bmatrix} \frac{\partial u}{\partial s} \\ \frac{1}{r} \frac{\partial v}{\partial \theta} + \frac{u}{r} \text{sen} \phi - \frac{w}{R_t} \\ \frac{1}{r} \frac{\partial u}{\partial \theta} + \frac{\partial v}{\partial s} - \frac{v}{r} \text{sen} \phi - \frac{n}{R_t} \frac{\partial v}{\partial s} \\ \theta_s + \frac{\partial w}{\partial s} \\ \theta_\theta + \frac{1}{r} \frac{\partial w}{\partial \theta} + \frac{v}{R_t} \end{Bmatrix} \quad (3)$$

Substituting the displacement field of eqn (1) in eqn (3) we can write the strain vector of eqn (3) as

$$\bar{\epsilon} = \begin{Bmatrix} \epsilon_m \\ 0 \end{Bmatrix} + \begin{Bmatrix} n \epsilon_b \\ \epsilon_s \end{Bmatrix} \quad (4)$$

where

$$\epsilon_m = \begin{Bmatrix} \frac{\partial u_0}{\partial s} \\ \frac{1}{r} \frac{\partial v_0}{\partial \theta} + \frac{u_0}{r} \text{sen} \phi - \frac{w_0}{r} \cos \phi \\ \frac{\partial v_0}{\partial s} + \frac{1}{r} \frac{\partial u_0}{\partial \theta} - \frac{v_0}{r} \text{sen} \phi \end{Bmatrix} \quad (5)$$

$$\epsilon_b = \left\{ \begin{array}{c} \frac{\partial \theta_s}{\partial s} \\ \frac{1}{r} \frac{\partial \theta_\theta}{\partial \theta} + \frac{\theta_s}{r} \sin \phi \\ \frac{\partial \theta_\theta}{\partial s} + \frac{1}{r} \frac{\partial \theta_s}{\partial \theta} - \frac{\theta_\theta}{r} \sin \phi - \frac{\cos \phi}{r} \frac{\partial v_0}{\partial s} \end{array} \right\}$$

$$\epsilon_s = \left\{ \begin{array}{c} \theta_s + \frac{\partial w_0}{\partial s} \\ \frac{1}{r} \frac{\partial w_0}{\partial \theta} + \frac{v_0}{r} \cos \phi \end{array} \right\}$$

are the generalized strain vectors due to membrane, bending and shear effects respectively. We have to note that in obtaining expressions (5) we have taken:

$$\left(1 + \frac{n}{R_t}\right) = 1; \quad \frac{n^2}{R_t} \frac{\partial \theta_\theta}{\partial s} \approx 0$$

and $r = R_t \cos \theta$.

Stresses. The resultant stresses vector corresponding with the generalised strains of eqn (5), can be written as

$$\sigma = \left\{ \begin{array}{c} \sigma_m \\ \sigma_b \\ \sigma_s \end{array} \right\} \quad (6)$$

where

$$\sigma_m = \left\{ \begin{array}{c} N_s \\ N_\theta \\ N_{s\theta} \end{array} \right\}; \quad \sigma_b = \left\{ \begin{array}{c} M_s \\ M_\theta \\ M_{s\theta} \end{array} \right\}; \quad \sigma_s = \left\{ \begin{array}{c} Q_s \\ Q_\theta \end{array} \right\} \quad (7)$$

are the resultant stresses vectors due to membrane, bending and shear effects respectively. (For sign convention see Fig. 1b.)

Stress/strain relationship. For an elastic material the relationship between generalised strains and resultant stresses can be easily written as

$$\sigma = D \epsilon \quad (8)$$

with

$$D = \begin{bmatrix} D_m & 0 \\ 0 & D_b \\ & D_s \end{bmatrix} \quad (9)$$

where for an isotropic material

$$D_m = \frac{Et}{1-\nu^2} \begin{bmatrix} 1 & \nu & 0 \\ \nu & 1 & 0 \\ 0 & 0 & \frac{1-\nu}{2} \end{bmatrix};$$

$$D_b = \frac{Et}{12(1-\nu^2)} \begin{bmatrix} 1 & \nu & 0 \\ \nu & 1 & 0 \\ 0 & 0 & \frac{1-\nu}{2} \end{bmatrix};$$

$$D_s = \frac{EtK}{2(1+\nu)} \begin{bmatrix} 1 & 0 \\ 0 & 1 \end{bmatrix} \quad (10)$$

where E is the Young modulus, ν the coefficient of Poisson, t the shell thickness and K a coefficient to take into account the warping of the section ($K = 5/6$ in rectangular sections).

Total potential energy of the shell. It is easy to show that the total potential energy of the shell can be written as

$$\Pi = \frac{1}{2} \iint_A \epsilon^T \sigma dA - \iint_A \mathbf{u}^T \mathbf{b} dA - \iint_A \mathbf{u}^T \mathbf{t} dA - \int_\Gamma \mathbf{u}^T \mathbf{p} d\Gamma \quad (11)$$

where \mathbf{u} is the displacement vector of a generic point of the shell middle surface. \mathbf{b} and \mathbf{t} are the body force and distributed loading vectors acting per unit area, \mathbf{p} is the vector of point loads acting along a line Γ and A the area of the shell middle surface.

Finite strip formulation for curved bridges. The bridge is divided into curved strips (see Fig. 2a). If we take k noded strips, the displacements field inside the strip, e ,

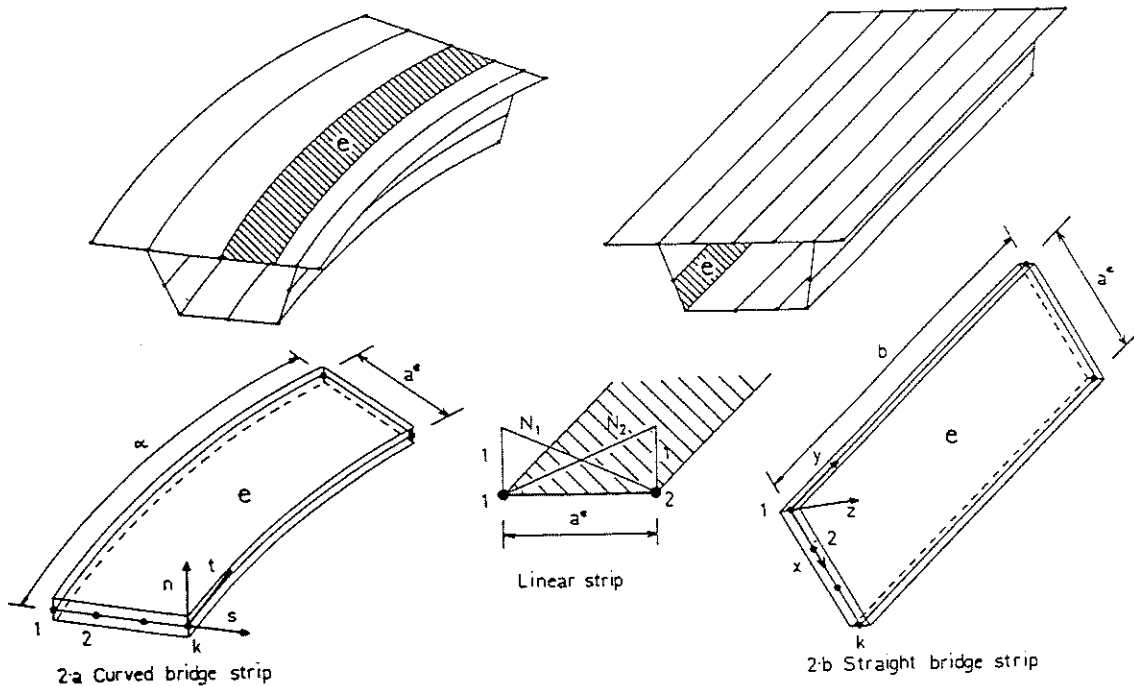


Fig. 2. Curved and straight bridges. Finite strip discretisations and local element coordinate axes.

can be expressed as products of polynomial shape functions in the transversal direction and Fourier expansions in the circular direction as

$$\mathbf{u}^{(e)} = \sum_{i=1}^K \sum_{l=1}^n \mathbf{N}_i^l \mathbf{a}_i^l \quad (12)$$

where \mathbf{N}_i^l and \mathbf{a}_i^l are, respectively, the generalised shape function matrix and the nodal displacement amplitudes vector associated with node i for the l th harmonic term. This matrices have the following form

$$\mathbf{u}^{(e)} = [u_0, v_0, w_0, \theta_s, \theta_\theta]^T \quad (13)$$

$$\mathbf{N}_i^l = \begin{bmatrix} N_i S_i & & & & \\ & N_i C_i & & & \\ & & N_i S_i & & \\ & & & N_i S_i & \\ 0 & & & & N_i C_i \end{bmatrix} \quad (14)$$

$$\mathbf{a}_i^l = [u_i^l, v_i^l, w_i^l, \theta_{s_i}^l, \theta_{\theta_i}^l]^T \quad (15)$$

where $S_i = \sin((l\pi\theta)/\alpha)$, $C_i = \cos((l\pi\theta)/\alpha)$ and α the bridge angle (see Fig. 2a).

It can be easily checked that the harmonic expansions chosen satisfy the conditions of simply supported strip for $\theta=0$ and $\theta=\alpha$. Thus, this formulation is valid for simply supported bridges with rigid diaphragms at the two ends.

The generalised strain vector can be obtained in terms of the nodal displacement amplitudes substituting eqn (12) in (4) to give

$$\boldsymbol{\epsilon} = \sum_i \sum_l \mathbf{B}_i^l \mathbf{a}_i^l \quad (16)$$

where \mathbf{B}_i^l is the generalised strain matrix for node i and the l th harmonic term, which it can be written as

$$\mathbf{B}_i^l = \begin{Bmatrix} \mathbf{B}_{mi}^l \\ \mathbf{B}_{bi}^l \\ \mathbf{B}_{si}^l \end{Bmatrix} \quad (17)$$

with

$$\mathbf{B}_{mi}^l = \begin{bmatrix} \frac{\partial N_i}{\partial s} S_i & 0 & 0 & 0 & 0 \\ \frac{N_i}{r} \sin \phi S_i & -\frac{N_i}{r} \frac{l\pi}{\alpha} S_i & -\frac{N_i}{r} \cos \phi S_i & 0 & 0 \\ \frac{N_i}{r} \frac{l\pi}{\alpha} C_i & \left(\frac{\partial N_i}{\partial s} - \frac{N_i}{r} \sin \phi \right) C_i & 0 & 0 & 0 \end{bmatrix}$$

$$\mathbf{B}_{bi}^l = \begin{bmatrix} 0 & 0 & 0 & \frac{\partial N_i}{\partial s} S_i & 0 \\ 0 & 0 & 0 & \frac{N_i}{r} \sin \phi S_i & -\frac{N_i}{r} \frac{l\pi}{\alpha} S_i \\ 0 & -\frac{\partial N_i}{\partial s} \frac{\cos \phi}{r} C_i & 0 & \frac{N_i}{r} \frac{l\pi}{\alpha} C_i & \left(\frac{\partial N_i}{\partial s} - \frac{N_i}{r} \cos \phi \right) C_i \end{bmatrix} \quad (18)$$

$$\mathbf{B}_{si}^l = \begin{bmatrix} 0 & 0 & \frac{\partial N_i}{\partial s} S_i & N_i S_i & 0 \\ 0 & \frac{N_i}{r} \cos \phi C_i & \frac{N_i}{r} \frac{l\pi}{\alpha} C_i & 0 & N_i C_i \end{bmatrix}$$

where \mathbf{B}_{mi}^l , \mathbf{B}_{bi}^l and \mathbf{B}_{si}^l are respectively, the generalised strain matrices due to membrane, bending and shear

effects for the node i and the l th harmonic term.

Expanding the force vectors in the same way as the displacement field we can write

$$(\mathbf{b}, \mathbf{t}, \mathbf{p}) = \sum_{l=1}^n (\mathbf{S}^l \mathbf{b}^l, \mathbf{S}^l \mathbf{t}^l, \mathbf{S}^l \mathbf{p}^l) \quad (19)$$

where

$$\mathbf{S}^l = \begin{bmatrix} S_i & & & & \\ & C_i & & & \\ & & S_i & & \\ 0 & & & S_i & \\ & & & & C_i \end{bmatrix} \quad (20)$$

and \mathbf{b}^l , \mathbf{t}^l and \mathbf{p}^l are the force amplitude vectors for the l th harmonic term.

Substituting eqns (8), (16), and (19) in the expressions of the total potential energy of the strip we can write

$$\begin{aligned} \Pi^e = & \frac{1}{2} \iint_{A^e} \left(\sum_{i=1}^n \sum_{l=1}^K \mathbf{B}_i^l \mathbf{a}_i^l \right)^T \mathbf{D} \left(\sum_{m=1}^n \sum_{j=1}^K \mathbf{B}_j^m \mathbf{a}_j^m \right) dA \\ & - \iint_{A^e} \left(\sum_{i=1}^n \sum_{l=1}^K \mathbf{N}_i^l \mathbf{a}_i^l \right)^T \sum_{m=1}^n \mathbf{b}^m dA \\ & - \iint_{A^e} \left(\sum_{i=1}^n \sum_{l=1}^K \mathbf{N}_i^l \mathbf{a}_i^l \right)^T \sum_{m=1}^n \mathbf{t}^m dA \\ & - \int_{\Gamma^e} \left(\sum_{i=1}^n \sum_{l=1}^K \mathbf{N}_i^l \mathbf{a}_i^l \right)^T \sum_{m=1}^n \mathbf{p}^m d\Gamma \end{aligned} \quad (21)$$

where all the integrals are evaluated over the strip area, A^e , or length Γ^e .

Taking into account the orthogonal properties of the functions S_i and C_i we can rewrite eqn (21) in a simplified form,

$$\Pi^e = \frac{1}{2} \sum_{i=1}^n \sum_{m=1}^n \sum_{l=1}^K \sum_{j=1}^K (\mathbf{a}_i^l)^T [\mathbf{K}_{ij}^{lm}]^e \mathbf{a}_j^m - \sum_{i=1}^n \sum_{l=1}^K (\mathbf{a}_i^l)^T [\mathbf{f}_i^l]^e \quad (22)$$

where

$$[\mathbf{K}_{ij}^{lm}]^e = \begin{cases} \frac{\alpha}{2} \int_0^{\alpha} (\bar{\mathbf{B}}_i^l)^T \mathbf{D} \bar{\mathbf{B}}_j^l r ds & \text{for } l=m \\ 0 & \text{for } l \neq m \end{cases} \quad (23)$$

is the stiffness matrix of the strip e of width a^e connecting nodes i and j for the l th harmonic term and

$$[f_i^l]^r = \iint_{A^c} (N_i^l)^T b^l dA + \iint_{A^c} (N_i^l)^T t^l dA + \int_{\Gamma^c} (N_i^l)^T p^l d\Gamma \quad (24)$$

with

$$B_i^{*l} = \bar{B}_i^l T_i^T \quad (29)$$

Matrix B_i^{*l} allows to evaluate directly the local resultant stresses from the global displacements as

$$\sigma = \sum_{l=1}^n \sum_{i=1}^K DB_i^{*l} \bar{a}_i^l \quad (30)$$

is the vector of forces for node, i , for the l th harmonic term. For more details about the load vector for different loading cases see Appendix 2.

In eqn (23) the matrix \bar{B}_i is identical to that of eqn (18) making $S_i = C_i = 1$.

We can see from eqns (23) and (24) that there is not coupling between the different harmonic terms and therefore the stiffness matrix and load vectors of the strip can be computed separately for each harmonic.

The discretised equilibrium equations for the whole structure can be easily obtained by minimising the total potential energy with respect to the nodal amplitude parameters which it leads to a system of equations of the form

$$\begin{bmatrix} K^{11} & & & \\ & K^{22} & & \\ & & \dots & \\ & & & K^{nn} \end{bmatrix} \begin{Bmatrix} a^1 \\ a^2 \\ \vdots \\ a^n \end{Bmatrix} = \begin{Bmatrix} f^1 \\ f^2 \\ \vdots \\ f^n \end{Bmatrix} \quad (25)$$

Therefore, the stiffness matrix K^l and the load vector f^l can be computed separately for each harmonic assembling the contributions from the different strips in the standard manner [31] and the system of equations for the l th harmonic term can be solved independently for the nodal amplitudes a^l . Repeating this process for all the harmonics, the different nodal amplitude parameters can be obtained and, subsequently, the displacements in each point of the structure can be computed by eqn (12) and the stresses by eqns (16) and (8).

Assembly of the stiffness matrices: Coordinate transformations. The assembly of the different stiffness matrices for the strips must be made in a global coordinate system. This can be easily done using the coordinate transformation matrix which relates the displacement and forces in the local and global systems as

$$\begin{aligned} \bar{a}_i &= T_i^c a_i \\ \bar{f}_i &= T_i^c f_i \end{aligned} \quad (26)$$

where the bar indicates the global system and T_i is the coordinate transformation matrix which expression can be seen in Fig. 3.

Thus, the different components of the strip stiffness matrix in the global system can be obtained as

$$[K_{ij}^l]^e = T_i [K_{ij}^l]^c [T_j^c]^T \quad (27)$$

or

$$[K_{ij}^l]^e = \frac{\alpha}{2} \int_0^{\alpha^c} (B_i^{*l})^T DB_j^{*l} r dr \quad (28)$$

The "reduced integration" two noded strip element for curved bridges. It is well known that to extend the applicability of Reissner-Mindlin theory for thin plate/shell situations the numerical overstiffening of the solution due to the shear effect as the thickness reduces must be eliminated. It has been extensively shown by many authors [11-17] that this can be easily done simply underintegrating the terms of the stiffness matrix due to shear using a numerical integration quadrature less than that needed for its exact integration, the remainder of the stiffness matrix being exactly integrated (selective integration). In a previous publication of the authors [18] it was shown how the linear strip plate element with just one Gauss point integration rule for the numerical integration of all terms of the stiffness matrix (reduced integration) behaves well in comparison with higher order strip elements for the static analysis of thick and thin plates.

Following these ideas, the reduced integration two noded strip element for curved bridges can be derived in a similar manner. From eqns (18) and (23) we can deduce that for an "exact" integration of the terms of the stiffness matrix a two points Gaussian integration rule should be used.†

Thus, for the reduced integration linear strip element one single integrating point suffices for all terms. This allows the stiffness matrix of eqn (23) to be obtained in a simple and explicit form as

$$[K_{ij}^l]^e = \frac{\alpha^c \alpha}{2} [\hat{B}_i^{*l}]^T \hat{D} \hat{B}_j^{*l} \quad (31)$$

where the "hat" indicates that the different terms are evaluated at the strip mid-point. An explicit form of matrix \hat{B}_i^{*l} is given in Appendix 1.

1.2 Straight bridges

The formulation can be easily derived from that for curved bridges presented in the previous section. Only details of the main differences between the two formulation will be given here.

Displacement field. For a plane "shell" element the three displacements of a point across the thickness can be expressed in terms of the displacements of the middle surface as

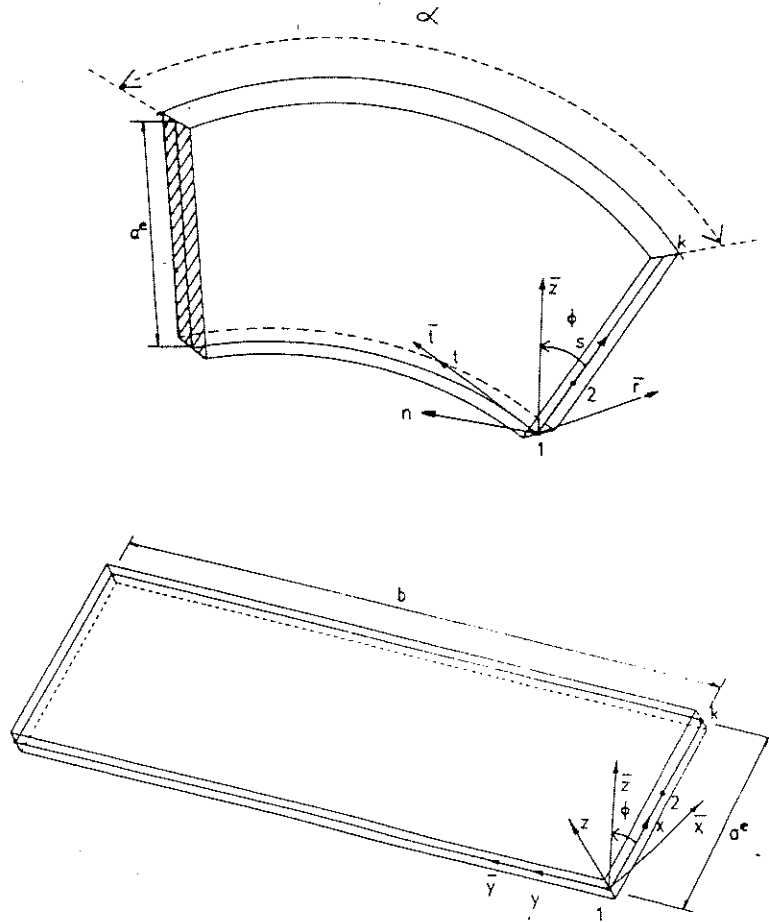
$$\begin{aligned} u(x, y, z) &= u_0(x, y) + z\theta_x(x, y) \\ v(x, y, z) &= v_0(x, y) + z\theta_y(x, y) \\ w(x, y, z) &= w_0(x, y) \end{aligned} \quad (32)$$

where all terms have the same meaning of those of eqn (1) the only difference being that now the constant local axes (x, y, z) replace the variable ones (s, t, n) .

Strain field. The strain vector can be easily obtained from standard elasticity theory as

$$\epsilon = \begin{Bmatrix} \epsilon_m \\ 0 \end{Bmatrix} + \begin{Bmatrix} z\epsilon_b \\ \epsilon_s \end{Bmatrix} \quad (33)$$

†This approximation implies that the logarithmic terms like $\log r_i/r_j$ which appear from the integration of some terms of the stiffness matrix have been approximated by $(2(r_j - r_i))/(r_j + r_i)$ where r_i and r_j are the radial distances of nodes i and j of the strip. Use of this approximation has given excellent results in practice as can be seen in the examples shown in this paper.



$$\bar{U}_i = T_i^e U_i$$

$$T_i^e = \begin{bmatrix} \text{Sen } \phi & 0 & -\text{Cos } \phi & 0 & 0 & 0 \\ 0 & 1 & 0 & 0 & 0 & 0 \\ \text{Cos } \phi & 0 & \text{Sen } \phi & 0 & 0 & 0 \\ 0 & 0 & 0 & 1 & 0 & 0 \\ 0 & 0 & 0 & 0 & \text{Sen } \phi & \text{Cos } \phi \\ 0 & 0 & 0 & 0 & -\text{Cos } \phi & \text{Sen } \phi \end{bmatrix}$$

Fig. 3. Transformation matrix for curved and straight strips.

where

$$\epsilon_m = \begin{Bmatrix} \frac{\partial u_0}{\partial x} \\ \frac{\partial v_0}{\partial y} \\ \frac{\partial u_0}{\partial y} + \frac{\partial v_0}{\partial x} \end{Bmatrix}; \quad \epsilon_b = \begin{Bmatrix} \frac{\partial \theta_x}{\partial x} \\ \frac{\partial \theta_y}{\partial y} \\ \frac{\partial \theta_x}{\partial y} + \frac{\partial \theta_y}{\partial x} \end{Bmatrix};$$

$$\epsilon_s = \begin{Bmatrix} \frac{\partial w}{\partial x} + \theta_x \\ \frac{\partial w}{\partial y} + \theta_y \end{Bmatrix} \quad (34)$$

are the corresponding generalised strain vectors for membrane, bending and shear. Note the decoupling of membrane and flexural effects at the element level, which it did not occur in the curved bridge formulation (see eqn 5).

Stresses. The expressions for the resultant stresses are identical to those of curved bridges (see eqn 6) simple

replacing s, θ and n by x, y and z respectively. Also the same sign criteria of Fig. 1b have been followed. The stress/strain relationship is identical to eqn (8).

Finite strip formulation for straight bridges. The displacement and strain field is expressed exactly in the same way as for curved bridges (see eqn 12) and eqn (16) simply replacing the angles α and θ for the bridge length b and the coordinate y respectively. (See Fig. 2b.) The strain matrix B_i^t , obtained from eqns (12) and (33), takes now the following form

$$B_i^t = [B_{mi}^t, B_{bi}^t, B_{si}^t]^T \quad (35)$$

where

$$B_{mi}^t = \begin{bmatrix} \frac{\partial N_i}{\partial x} S_i & 0 & 0 & 0 & 0 \\ 0 & -N_i \frac{l\pi}{b} S_i & 0 & 0 & 0 \\ \frac{l\pi}{b} C_i & \frac{\partial N_i}{\partial x} C_i & 0 & 0 & 0 \end{bmatrix}$$

$$\mathbf{B}_{b_i}^l = \begin{bmatrix} 0 & 0 & 0 & \frac{\partial N_i}{\partial x} S_i & 0 \\ 0 & 0 & 0 & 0 & -N_i \frac{l\pi}{b} S_i \\ 0 & 0 & 0 & N_i \frac{l\pi}{b} C_i & \frac{\partial N_i}{\partial x} C_i \end{bmatrix} \quad (36)$$

$$\mathbf{B}_{s_i}^l = \begin{bmatrix} 0 & 0 & \frac{\partial N_i}{\partial x} S_i & N_i S_i & 0 \\ 0 & 0 & N_i \frac{l\pi}{b} C_i & 0 & N_i C_i \end{bmatrix}$$

are respectively the membrane, bending and shear strain matrices for node i and the l th harmonic term.

It is worth noting that matrix \mathbf{B}_i^l for straight bridges can be directly obtained from that for curved bridges (see eqn 17), simply substituting in eqn (18) α by b/r , with r being now a large number.

Following the same steps that for curved bridges the decoupled stiffness matrix for the l th harmonic term can be obtained by

$$[\mathbf{K}_{ij}^{ll}]^e = \frac{b}{2} \int_0^{a^e} [\bar{\mathbf{B}}_i^l]^T \mathbf{D} \bar{\mathbf{B}}_j^l dx \quad (37)$$

The expression for the loading vector \mathbf{f}_i^l is identical to that of eqn (24).

Transformation of the stiffness matrix to the global axes can be done exactly in the same way as explained for curved bridges. Moreover, if linear reduced integrated strip elements are used, the stiffness matrix can be evaluated explicitly with just one integrating Gauss point to give

$$[\mathbf{K}_{ij}^{ll}]^e = \frac{a^e b}{2} [\hat{\mathbf{B}}_i^{*l}]^T \hat{\mathbf{D}} \hat{\mathbf{B}}_j^{*l} \quad (38)$$

where the “*” indicates again values at the center of the strip and $\hat{\mathbf{B}}_i^{*l}$ is obtained by eqn (29).

An explicit form of matrix $\hat{\mathbf{B}}_i^{*l}$ can be seen in Appendix I. Note the useful analogy, already mentioned, which it allows to derive all the relevant matrices for straight bridges from the corresponding expressions for curved bridges.

1.3 Curved and straight plates

The general formulation for the analysis of curved and straight plates can be directly derived from the formulation for curved and straight bridges presented in 1.1 and 1.2 simply neglecting in all equations the membrane behaviour of the structure. Therefore, expanding the three main displacement variables, w , θ_x and θ_y in the same way as described for curved and straight bridges in eqns (12) and (16), the corresponding finite strip plate formulations can be obtained in a straightforward manner.

Details of the formulation follow precisely the same steps explained in 1.1 and they will not be repeated here. The global strip stiffness matrix and load vectors for the l th armonic term are obtained by eqn (23) or (37) with the strain matrix $\bar{\mathbf{B}}_i^l$ being now given by

Curved plate

$$\bar{\mathbf{B}}_i^l = \begin{bmatrix} 0 & \frac{\partial N_i}{\partial s} & 0 \\ 0 & \frac{N_i}{r} \sin \phi & -\frac{N_i l\pi}{r \alpha} \\ 0 & \frac{N_i l\pi}{r \alpha} & \frac{\partial N_i}{\partial s} - \frac{N_i}{r} \sin \phi \\ \frac{\partial N_i}{\partial s} & N_i & 0 \\ \frac{N_i l\pi}{r \alpha} & 0 & N_i \end{bmatrix};$$

Straight plate

$$\bar{\mathbf{B}}_i^l = \begin{bmatrix} 0 & \frac{\partial N_i}{\partial x} & 0 \\ 0 & 0 & -N_i \frac{l\pi}{b} \\ 0 & N_i \frac{l\pi}{b} & \frac{\partial N_i}{\partial x} \\ \frac{\partial N_i}{\partial x} & N_i & 0 \\ N_i \frac{l\pi}{b} & 0 & N_i \end{bmatrix} \quad (39)$$

If again the one point reduced integration two noded strip is used an explicit form of all the matrices can be easily obtained (see Appendix 1).

2. AXISYMMETRIC SHELLS

The formulation for axisymmetric shells follows very closely the steps of Section 1 for curved bridges. For shells under arbitrary loading the displacement, strain and stress fields are identical to those expressed in eqns (1)–(10) and the total potential energy expression corresponds with that of eqn (11), the only difference being that the integrals are now taken over a whole circumference.

The discretized displacement field inside each shell strip can be expressed in terms of the symmetrical and anti-symmetrical contributions of the deformation as

$$\mathbf{u} = \sum_{l=0}^n \sum_{i=1}^K (N_i^l + \bar{N}_i^l) \mathbf{a}_i^l \quad (40)$$

where

$$\mathbf{u} = [u_0, v_0, w_0, \theta_s, \theta_\theta]^T \quad (41)$$

$$\mathbf{a}_i^l = [u_{0p}, v_{0p}, w_{0p}, \theta_{sp}, \theta_{\theta p}]^T \quad (42)$$

are the displacement and nodal parameter vectors, and

$$\mathbf{N}_i^l = \begin{bmatrix} N_i C_l & & & & \\ & N_i S_l & & & \\ & & N_i C_l & & \\ 0 & & & N_i C_l & \\ & & & & N_i S_l \end{bmatrix};$$

$$\bar{\mathbf{N}}_i^l = \begin{bmatrix} N_i S_l & & & & \\ & N_i C_l & & & \\ & & N_i S_l & & \\ 0 & & & N_i S_l & \\ & & & & N_i C_l \end{bmatrix} \quad (43)$$

are the shape function matrices corresponding to symmetrical and anti-symmetrical displacement fields, $S_i = \sin l\theta$ and $C_i = \cos l\theta$.

To simplify the computations it is usual to evaluate the contributions of an arbitrary non-symmetric load as sum of a symmetrical and an anti-symmetrical part. Therefore, we will restrict ourselves here to the study of the case in which all the loads are symmetrical with respect to a plane (which for simplicity we will take as that of $\theta = 0$ in Fig. 12) which implies that only matrix N_i^l of eqn (43) will be used. The study of the anti-symmetric case would be identical taking matrix \bar{N}_i^l instead of N_i^l and will not be presented here.

Therefore, the symmetrically acting loads will be expanded in the form

$$(\mathbf{b}, \mathbf{t}, \mathbf{p}) = \sum_{l=0}^n (S_l \mathbf{b}^l, S_l \mathbf{t}^l, S_l \mathbf{p}^l) \quad (44)$$

where

$$S_l = \begin{bmatrix} C_l & & & & & \\ & S_l & & & & \\ & & C_l & & & \\ & & & C_l & & \\ 0 & & & & C_l & \\ & & & & & S_l \end{bmatrix} \quad (45)$$

and all the other vectors have been defined previously.

Following exactly the same steps that those explained in eqns (12)–(24) for the curved bridge case, we can arrive easily to the decoupled system of stiffness equations for each harmonic term where the stiffness matrix is now given by

$$\begin{aligned} [\mathbf{K}_{ij}^{ll}]^c &= 2\pi \int_0^{a^c} \bar{\mathbf{B}}_i^{lT} \mathbf{D} \bar{\mathbf{D}}_j^l r dr \quad \text{for } l=0 \\ [\mathbf{K}_{ij}^{ll}]^r &= \pi \int_0^{a^r} \bar{\mathbf{B}}_i^{lT} \mathbf{D} \bar{\mathbf{D}}_j^l r dr \quad \text{for } l \neq 0 \end{aligned} \quad (46)$$

with the generalized strain matrix defined by

$$\bar{\mathbf{B}}_i^l = [\bar{\mathbf{B}}_{m_i}^l, \bar{\mathbf{B}}_{b_i}^l, \bar{\mathbf{B}}_{s_i}^l]^T \quad (47)$$

where

$$\begin{aligned} \bar{\mathbf{B}}_{m_i}^l &= \begin{bmatrix} \frac{\partial N_i}{\partial s} & 0 & 0 & 0 & 0 \\ N_i \frac{\sin \phi}{r} & \frac{N_i}{r} l & -N_i \frac{\cos \phi}{r} & 0 & 0 \\ -\frac{N_i}{r} l & \left(\frac{\partial N_i}{\partial s} - \frac{N_i}{r} \sin \phi \right) & 0 & 0 & 0 \end{bmatrix} \\ \bar{\mathbf{B}}_{b_i}^l &= \begin{bmatrix} 0 & 0 & 0 & \frac{\partial N_i}{\partial s} & 0 \\ 0 & 0 & 0 & \frac{N_i}{r} \sin \phi & \frac{N_i}{r} l \\ 0 & -\frac{\partial N_i}{\partial s} \frac{\cos \phi}{r} & 0 & \frac{N_i}{r} l & \left(\frac{\partial N_i}{\partial s} - \frac{N_i}{r} \sin \phi \right) \end{bmatrix} \\ \bar{\mathbf{B}}_{s_i}^l &= \begin{bmatrix} 0 & 0 & \frac{\partial N_i}{\partial s} & N_i & 0 \\ 0 & \frac{N_i}{r} \cos \phi & -\frac{N_i}{r} l & 0 & N_i \end{bmatrix} \end{aligned} \quad (48)$$

are the corresponding membrane, bending and shear strain matrices.

Transformation of the element stiffness matrix into a global coordinate system follows precisely the same steps than those explained in eqns (26)–(30) for curved bridges, with the transformation matrix \mathbf{T}_i^c being identical to that defined in Fig. 3, and they will not be repeated here.

If the reduced integration two noded strip element is used, one Gauss point again suffices for the evaluation of all integrals and an explicit form of the stiffness matrix can be simply obtained. Details of these expressions and of those for the loading vector \mathbf{t}_i^l for different load cases are given in Appendices 1 and 2. It is interesting to note that eqns (48) for the different components of matrix $\bar{\mathbf{B}}_i^l$ can be directly obtained from the analogous expressions for curved bridges, simply substituting, in eqn (18) $l\pi/\alpha$ by $-l$ and making $S_l = C_l = 1$. This shows again the versatility of the general formulation and how it allows to treat bridges, plates and axisymmetric shells in a unified manner.

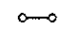
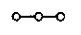
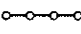
If the loading is also axisymmetric the same formulation is directly applicable simply evaluating the contribution of the zero harmonic term (i.e. making $l=0$ in eqns 48). However, a simpler formulation can be automatically derived taking into account only the contributions of the non zero displacements u , w and θ_s in matrix \mathbf{B}_i^0 . This formulation was originally presented by Zienkiewicz *et al.* [20] who were the first in suggesting the use of the reduced integration linear axisymmetric shell element for this kind of problems.

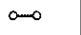
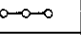
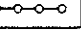
Zero energy nodes. It is well known that the use of reduced integration techniques can, sometimes, excite spurious zero energy modes in a single element which, if they are compatible within a certain mesh they can propagate and pollute the numerical solution. This fact is of extreme importance, in particular for dynamic problems where small oscillations in the solution, not always detectable in the static case, can be largely amplified. One of the ways of detecting if a single element, or mesh of elements, has spurious zero energy nodes is performing a check in the number of zero eigenvalues of the stiffness matrix. Any extra zero eigenvalue over the number of degrees of freedom needed to restrain the element from rigid body movement, is associated with a possibly propagable zero energy mode.

In Table 1 the number of extra zero eigenvalues of matrix \mathbf{K}^{11} and \mathbf{K}^{00} over the number of rigid body modes for a single linear, quadratic and cubic bridge, plate and axisymmetric shells strip element using different integration rules are presented. We can see that for the bridge and plate strip (both straight and curved) only the linear strip element with the reduced integration rule presents a spurious zero mode. This mode, however, disappears if a mesh of two or more elements are considered and the element can be considered as "safe" in this context. For axisymmetric shells, however, the linear element presents with all integrating rules a spurious zero mode. It has been checked that for the static case this mode is not propagable in a mesh of two or more elements. This is not so in the dynamic case and wrong oscillatory solutions can sometimes be obtained. Use of the quadratic or cubic elements in this case overcomes this problem.

In conclusion, all strip elements can be considered as safe in the context of the static analysis of bridges, plates and axisymmetric shell structures. The same applies for the dynamic analysis of bridges and plates. For axisymmetric shells, however, the linear element is un-

Table 1. Integration rules and number of zero eigenvalues of matrix K'' for different strip elements

GAUSSIAN INTEGRATION RULES			
STRIP ELEMENT	FULL (F)	SELECTIVE(S)	REDUCED (R)
	K_b'' K_s''	K_b'' K_s''	K_b'' K_s''
	2 2	2 1	1 1
	3 3	3 2	2 2
	4 4	4 3	3 3

NUMBER OF EXTRA ZERO EIGENVALUES IN A SINGLE ELEMENT						
STRIP ELEMENT	BRIDGE AND PLATE STRIP K''			AXISYMMETRIC SHELL ELEMENT K^{00}		
	F	S	R	F	S	R
	0	0	1*	1+	1+	1+
	0	0	0	0	0	0
	0	0	0	0	0	0

* Non propagable in a mesh of two or more elements

+ Only propagable in the dynamic case.

reliable due to the existence of an easily propagable zero energy mode. Considerable effort has been put recently in trying to "incorporate" the linear element for axisymmetric shell dynamic analysis. Thus, Ohayon and Nicollas-Vullierme have shown how the use of a mixed formulation can eliminate the spurious oscillations[29]. Use of other possibilities within the displacement formulation, like the use of internal hierarchical variables seem promising and are currently being investigated. The subject, however, falls outside the objectives of this paper where we are restricted only to the static case. Results which show the versatility of the general formulation and the performance of the linear strip element in this context for a variety of problems will be shown in the next sections.

Example 1. Simple supported square plate. Convergence study

In this example two simple supported square plates under uniformly distributed loading with thickness/width ratios of 0.1 and 0.01 respectively have been analysed with different meshes of linear strip elements using full, selective and reduced integration. Only half of the plate has been analysed due to symmetry. Numerical results obtained can be seen in Fig. 4, where the nondimensional values of the deflection and bending moments at the center of the plate vs the number of strips have been plotted. Results obtained using reduced or selective integration with 9 non zero harmonic terms were identical. Also, convergence of the solution in this case is very fast for both plate thickness. Use of full integration, however, leads to poor convergence in the thick plate case and to meaningless results in the thin one as expected. Similar results have been obtained for a wide range of plate thicknesses (so far till $t/L = 10^{-7}$) which prove the good behaviour of the linear strip element for thick and very thin plate analysis. More information can be found in Ref. [18].

Example 2. Curved plate: Slab model of Coull and Das

This example shows the accuracy of the linear strip element for curved plate analysis. The example chosen is a curved thin plate simply supported at the two ends under a point load for which experimental and numerical results are available. The geometry of the plate, material properties, loading position and finite strip mesh used in the analysis can be seen in Fig. 5. Results for the deflection along the center of the plate obtained with the reduced integrating linear element using 25 non zero harmonic terms can be seen in the same figure where experimental and theoretical results obtained by Coull and Das[21], finite strip solutions based on Kirchhoff's theory obtained by Thorpe[22] and Cheung[6] and finite element solutions reported by Sawko and Meriman[23] and Fam and Turkstra[24] for the same problem are also shown for comparison.

Accuracy of the linear strip element is again noticeable.

Example 3. Straight bridge: Simple supported concrete slab/beam bridge over the motorway Nueve de Julio (Buenos Aires)

This example tries to show the adequacy of the linear strip element for practical bridge deck analysis. The example chosen is one of the bridges of the urban motorway Nueve de Julio actually under construction in the City of Buenos Aires (Argentina). The geometry of the structure, loading position, material properties and finite strip discretisation used in the analysis can be seen in Fig. 6. Numerical results for the vertical deflection; transverse bending moment and longitudinal resultant stress in the slab at the mid section obtained with 15 non zero harmonic terms have been plotted in Fig. 7. The corresponding diagrams shown in the same figure have been extrapolated from the finite strip results which have been marked with a circle. To assess the validity of the numerical solution, an equilibrium check has been

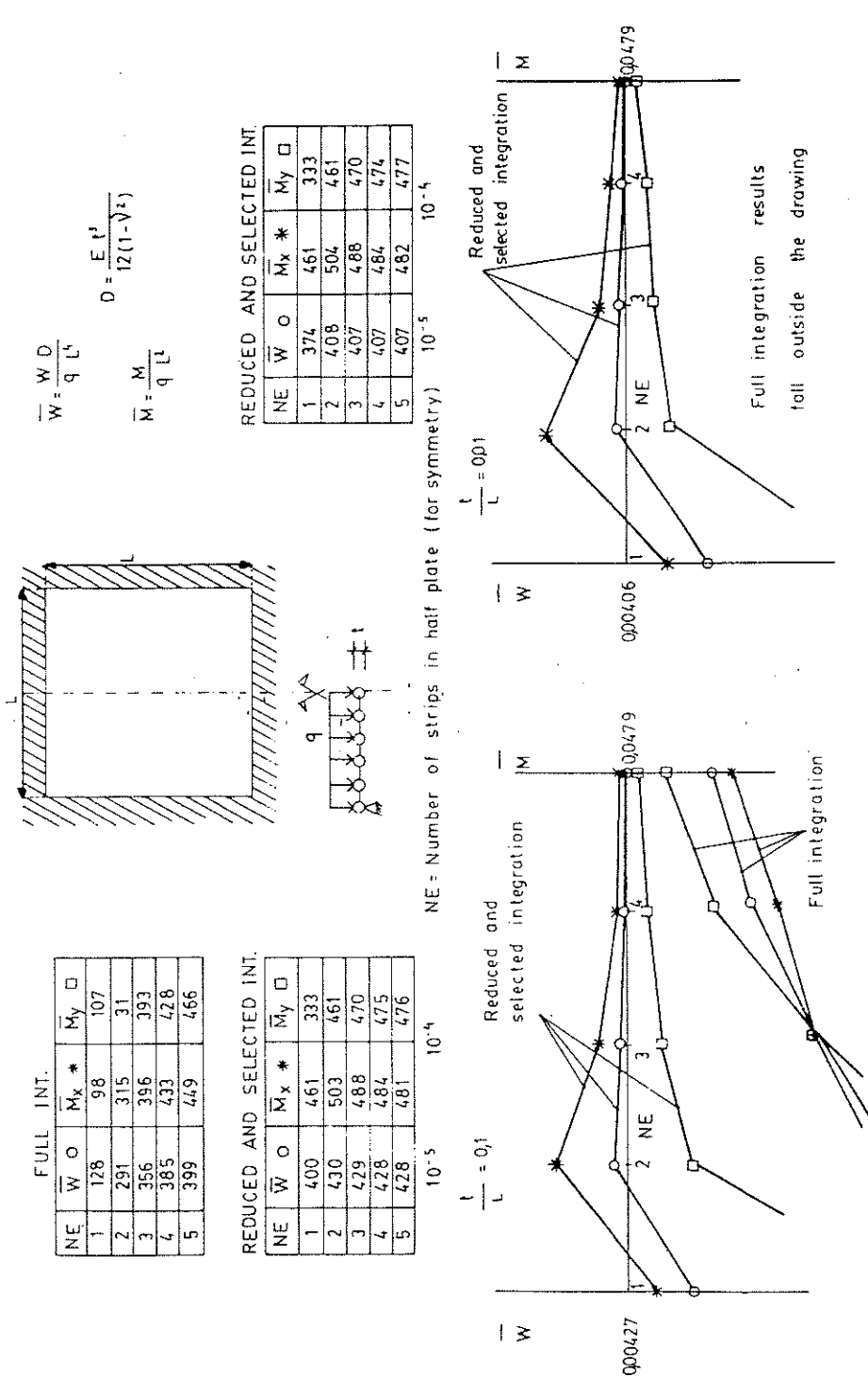


Fig. 4. Square plate under uniformly distributed loading. Convergence of the linear strip with full, selective and reduced integration for $t/L = 0.1$ and 0.01 .

12 Elements

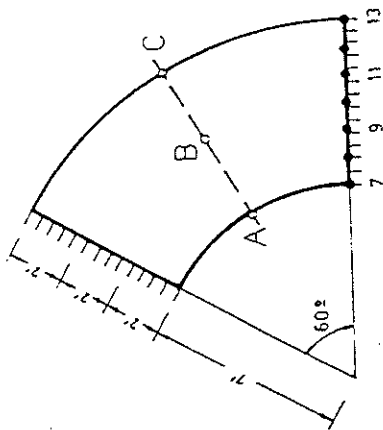
8 Non zero harmonics

$E = 42.460 \text{ lb/inch}^2$

$\nu = 0.3$

$t = 0.172'$

Loading: Point load of 1lb acting in A, B, C.



Loading Position	Rad. inc.	COULL & DAS		FINITE STRIP			FINITE ELEMENT		
		Experi.	Theor.	Thorpe	Cheung	*	Sawko	Fam & Turkst	
A	13	0.876	0.750	0.882	0.995	0.878	0.851	0.880	0.881
	11	0.578	0.500	0.587	0.674	0.581	0.559	0.577	0.578
	9	0.353	0.300	0.356	0.388	0.357	0.344	0.353	0.354
B	7	0.194	0.180	0.195	0.206	0.195	0.192	0.193	0.194
	13	0.457	0.470	0.459	0.441	0.460	0.445	0.456	0.457
	11	0.342	0.370	0.363	0.379	0.348	0.333	0.342	0.343
C	9	0.241	0.250	0.242	0.222	0.247	0.236	0.241	0.241
	7	0.155	0.170	0.156	0.147	0.158	0.154	0.154	0.158
	13	0.195	0.150	0.195	0.180	0.195	0.192	0.193	0.194
Reference	11	0.163	0.135	0.165	0.152	0.167	0.162	0.163	0.164
	9	0.157	0.125	0.153	0.149	0.155	0.151	0.151	0.151
	7	0.169	0.145	0.170	0.173	0.173	0.170	0.169	0.169
			21	22	6		23	24	

* LINEAR MINDLIN STRIP ELEMENT WITH REDUCED INTEGRATION

Fig. 5. Slab model of Coull and Das: Results for the deflection along ABC obtained by several authors.

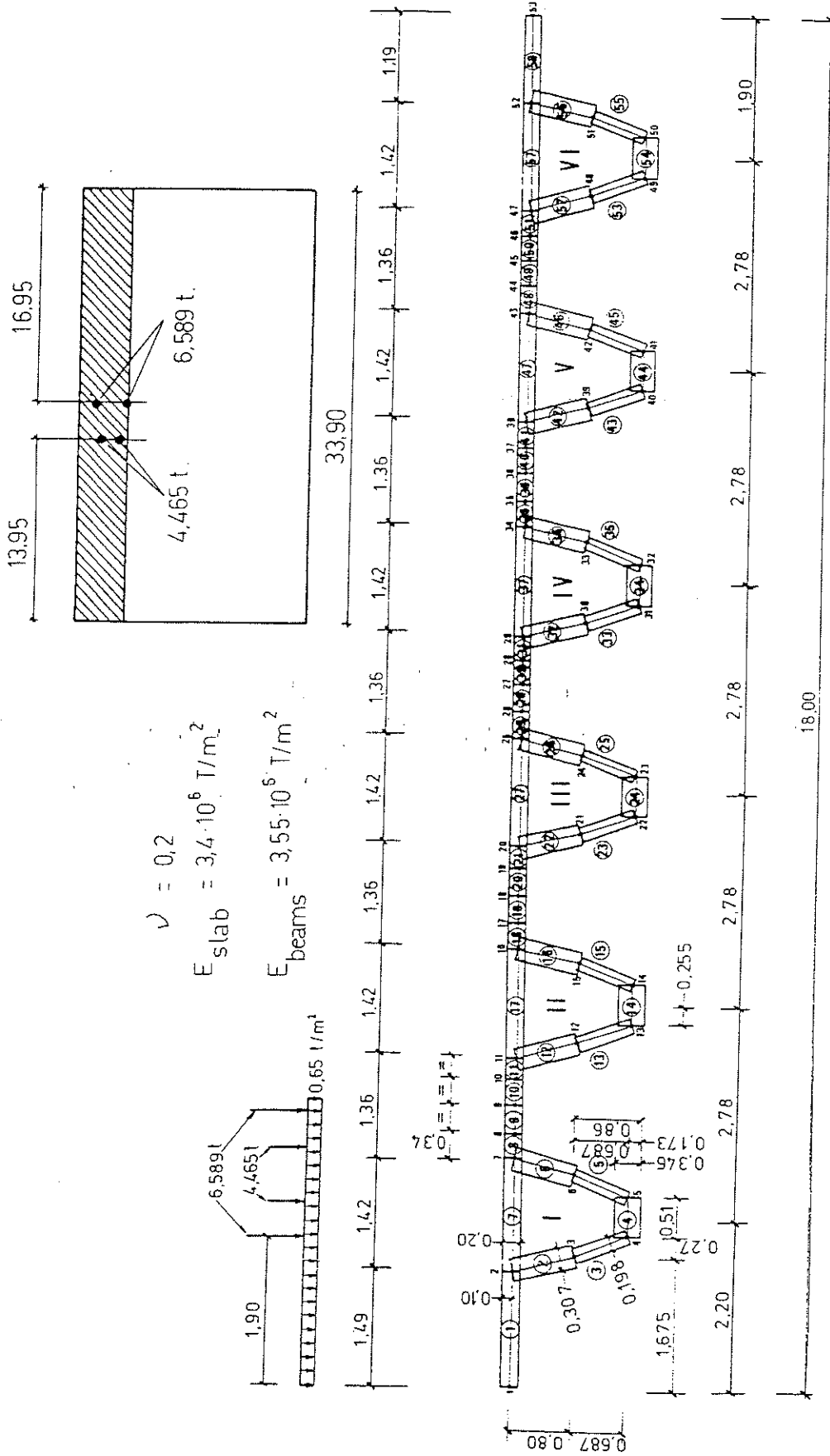


Fig. 6. Simple supported concrete bridge: Geometry of structure, loading position and finite strip idealisation in 58 linear strips.

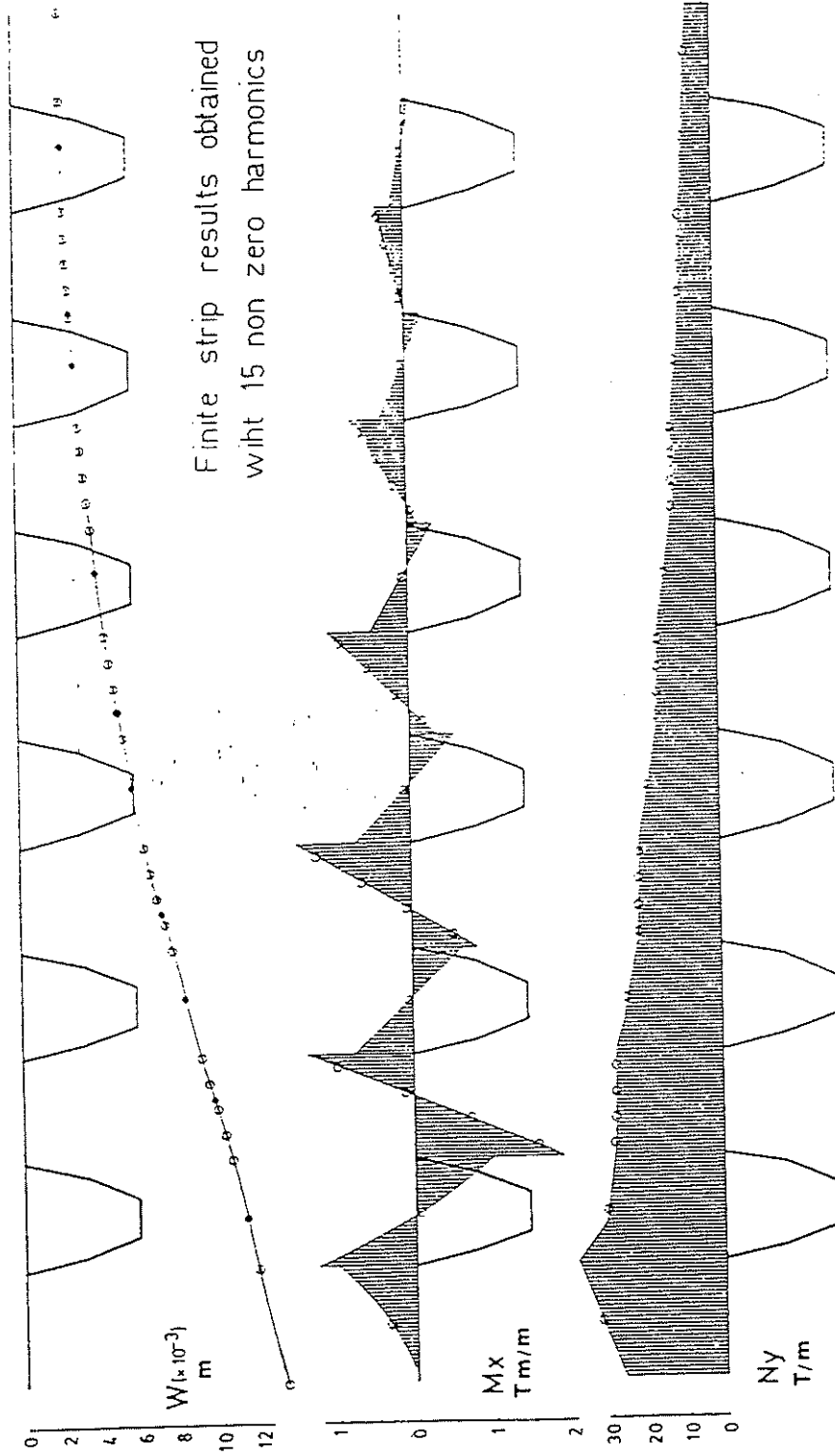


Fig. 7. Curves for the deflection, w , transverse bending moment, M_x , and longitudinal resultant stress, N_y , in the slab at the bridge mid section.

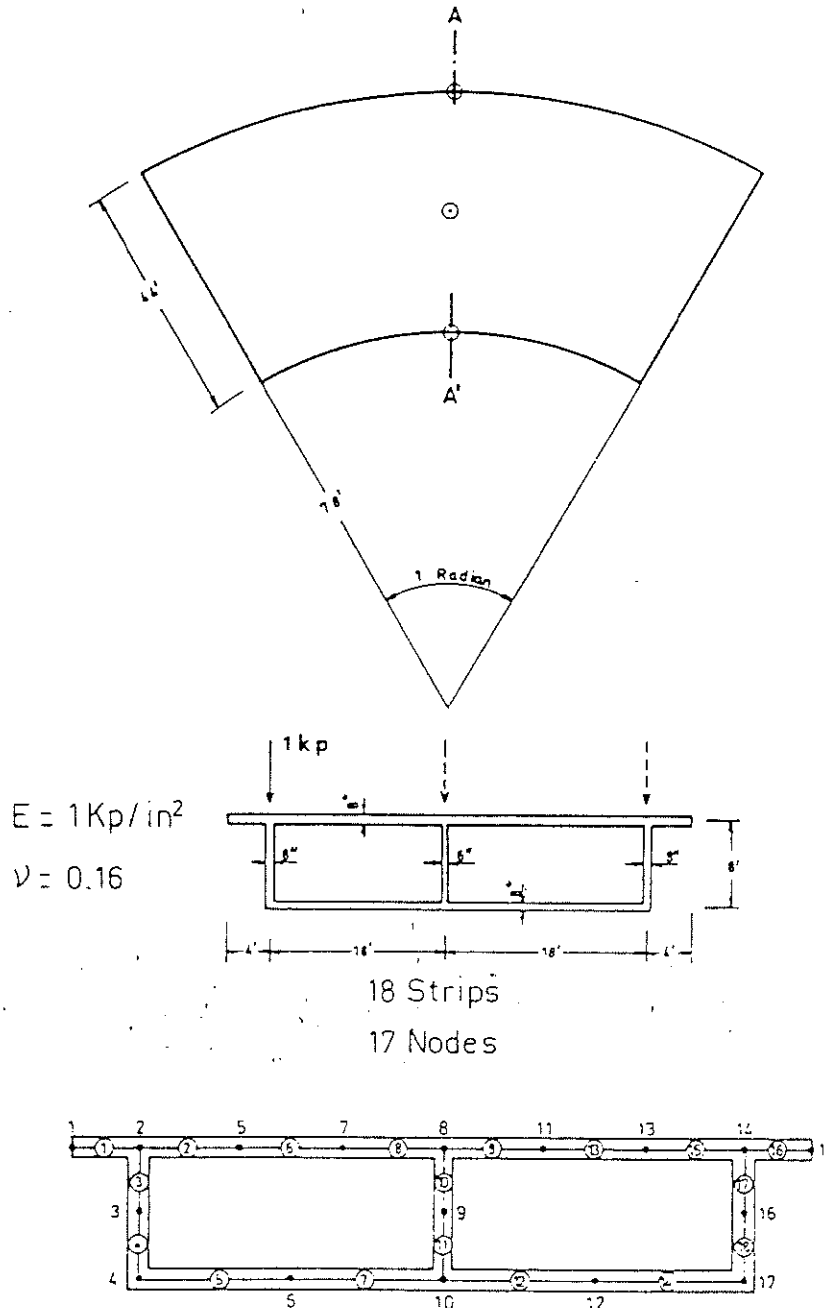


Fig. 8. Curved box girder bridge: Geometry of the structure and finite strip idealisation into 18 strips.

performed comparing the total longitudinal bending moment in the mid section with the value obtained by using simple beam theory. The percentage of error obtained has been less than 2%, which can be considered as good for practical design purposes.

Example 4. Curved bridge: Model of Cheung

The example chosen to check the behaviour of the linear strip element for curved bridge analysis is a simple supported box girder bridge of circular plant under a point load acting in the mid section over one of the webs. The geometry of the structure, material properties and finite strip mesh of 18 elements used in the analysis can be seen in Fig. 8. This problem has also been analyzed by Cheung using a Kirchhoff strip formulation[6]. Results for the horizontal and vertical displacements in the mid webs section for three different positions of the point load are shown in Fig. 9. In Fig. 10 the axial resultant

stress and the radial and circumferential bending moments have been plotted together with some of the Cheung results which are shown for comparison. 15 non zero harmonic terms have been used in the analysis.

Example 5. Axisymmetric shells: Circular plate under eccentric point load

The reduced integration two noded axisymmetric shell element has already been proved to behave extremely well for the static analysis of axisymmetric shells under axisymmetrical loading[20]. In this paper we have shown how axisymmetric shells can be easily treated as a particular case of a more general curved shell formulation. To show the accuracy of the element in the context of the analysis of this type of structures two simple demonstrative examples have been chosen. The first is a thin circular plate under a point load acting at a certain distance from the center of the plate. The example is

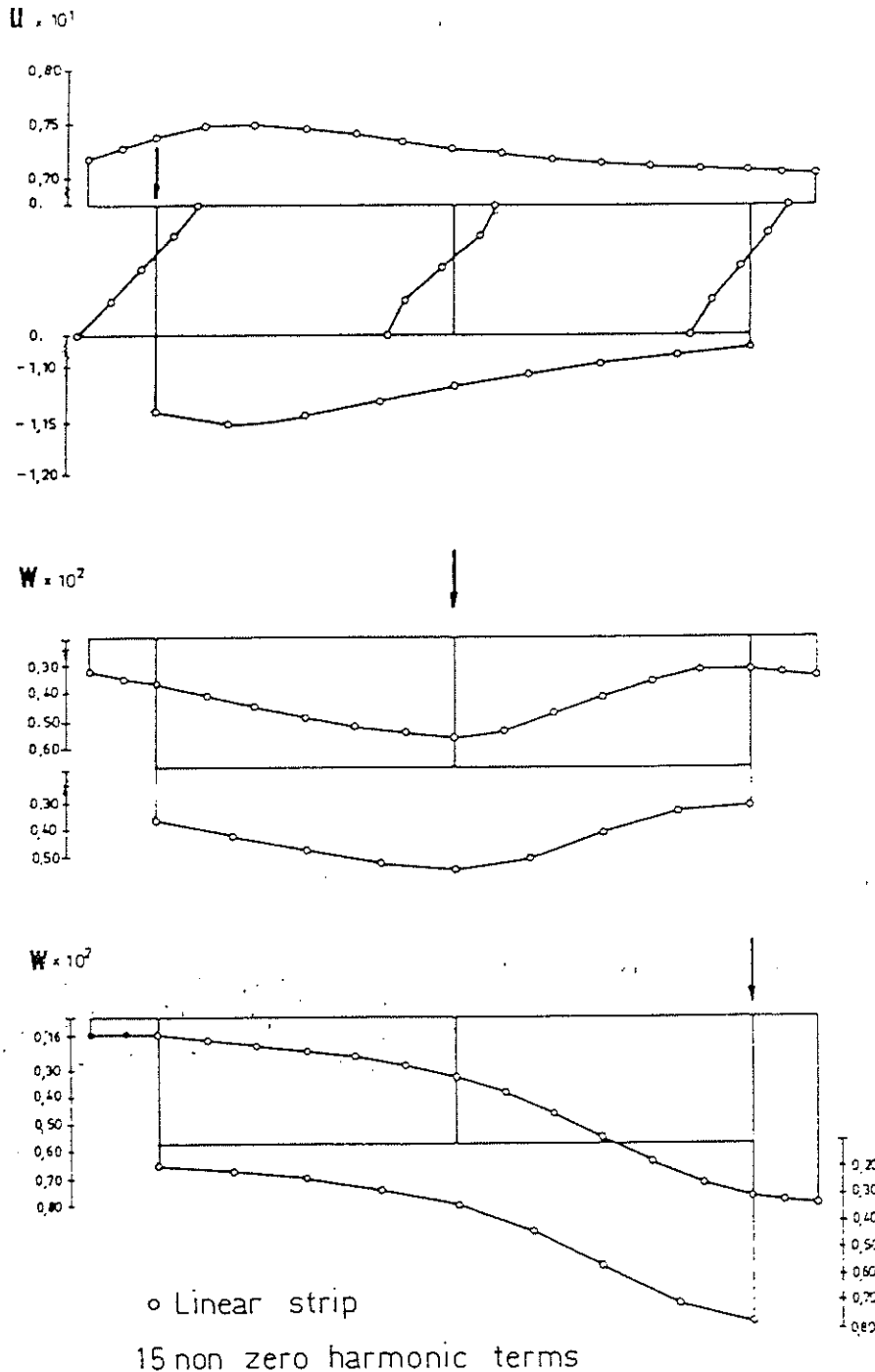


Fig. 9. Curved box girder bridge: Displacements at the mid section for several loading positions.

fully described in Fig. 11, where results for the deflection, and radial bending moment along several sections obtained with the linear axisymmetric element and with a mesh of 8 noded isoparametric reduced integrated Mindlin plate finite elements[13] have been shown for comparison. The Timoshenko "exact" thin plate solution[32] for the deflection under the load has been also plotted. Accuracy of the linear element is again good.

Example 6. Axisymmetric shells: Pinched cylindrical shell

The last example is the classical thin cylindrical shell under two point loads acting diametrically opposed. The cylinder has rigid diaphragms at the two end sections (see Fig. 12). This example, well known in the shell

literature, has been solved by several authors. Amongst others, there is an "exact" analytical double series solution due to Flugge[26], Finite element solutions have been reported by Oñate *et al.*[16], Lindberg *et al.*[27], Ahmad *et al.*[28], and many others. The solution here presented is probably the simplest one using only 20 linear axisymmetric shell elements. Nevertheless is highly accurate as it is demonstrated in Fig. 11 where the linear element results for the displacements and axial forces along several sections using 15 non zero harmonic terms compare well vs more sophisticated analytical and finite element solutions.

CONCLUSIONS

In this paper it has been shown how plates, bridges and axisymmetric shells of uniform transverse cross

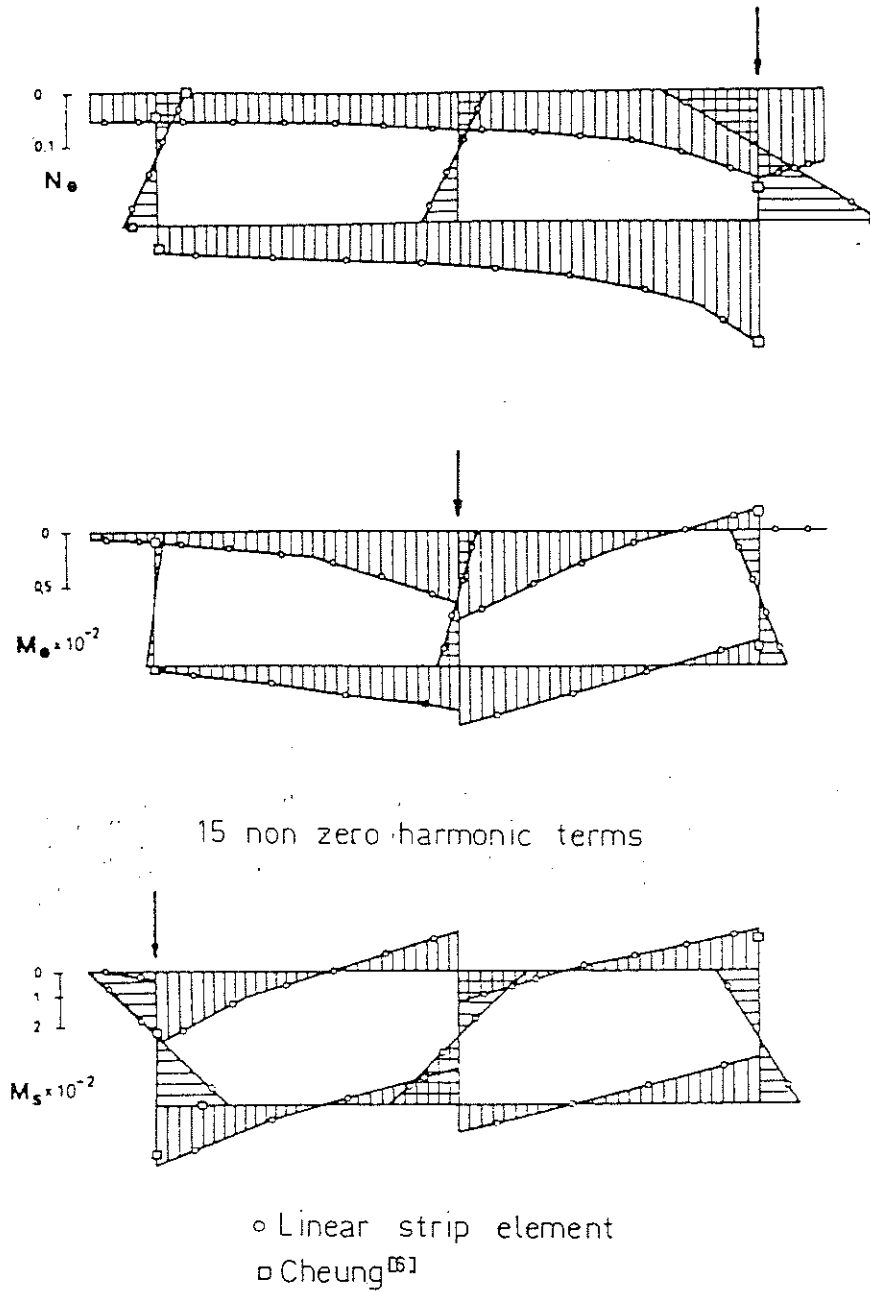


Fig. 10. Curved box girder bridge: Circumferential resultant stress, N_θ , and bending moments M_x and M_y at the central section.

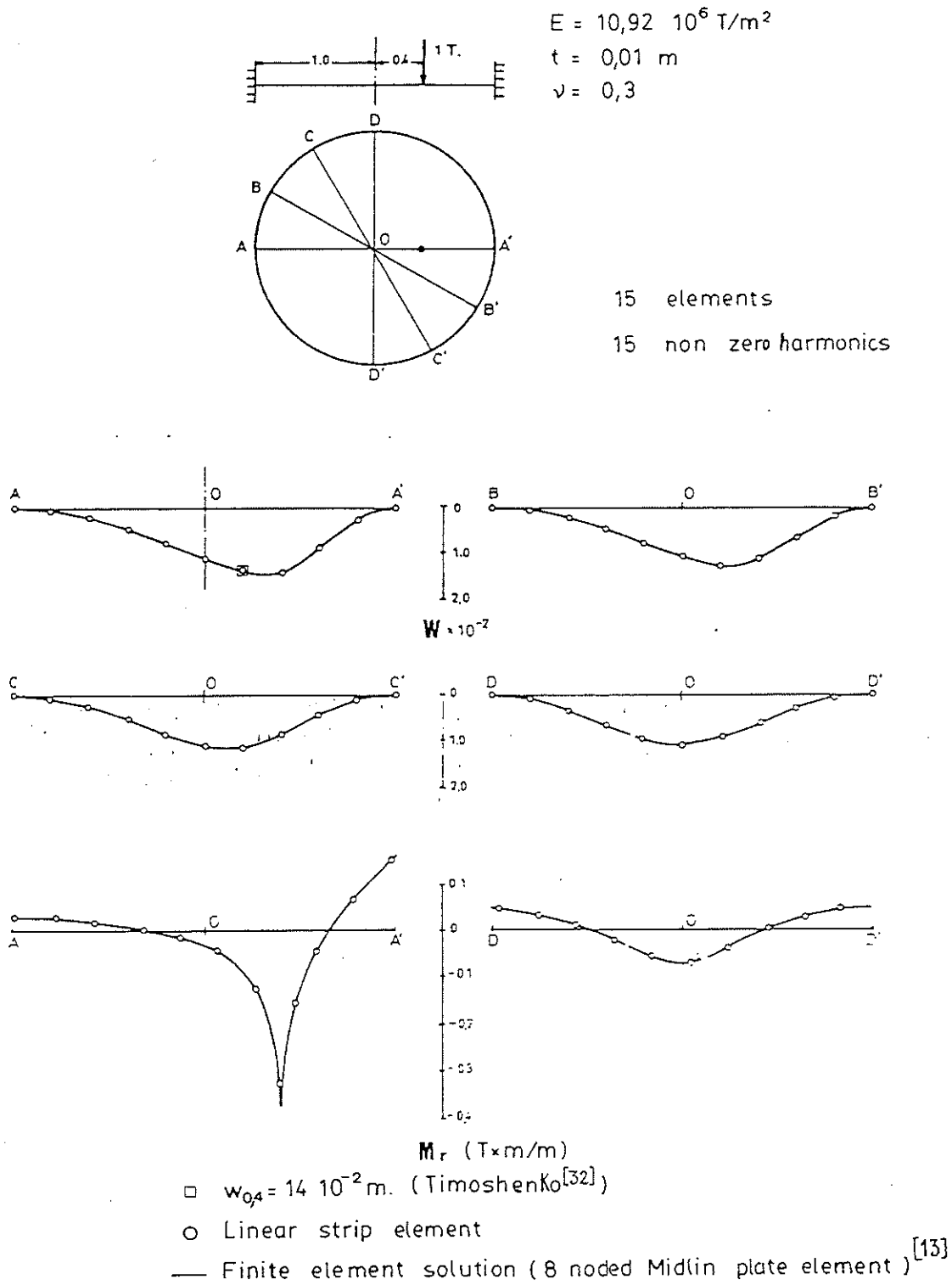


Fig. 11. Circular thin plate under point load. Vertical deflections w , and radial bending moment, M_r , distributions along several sections.

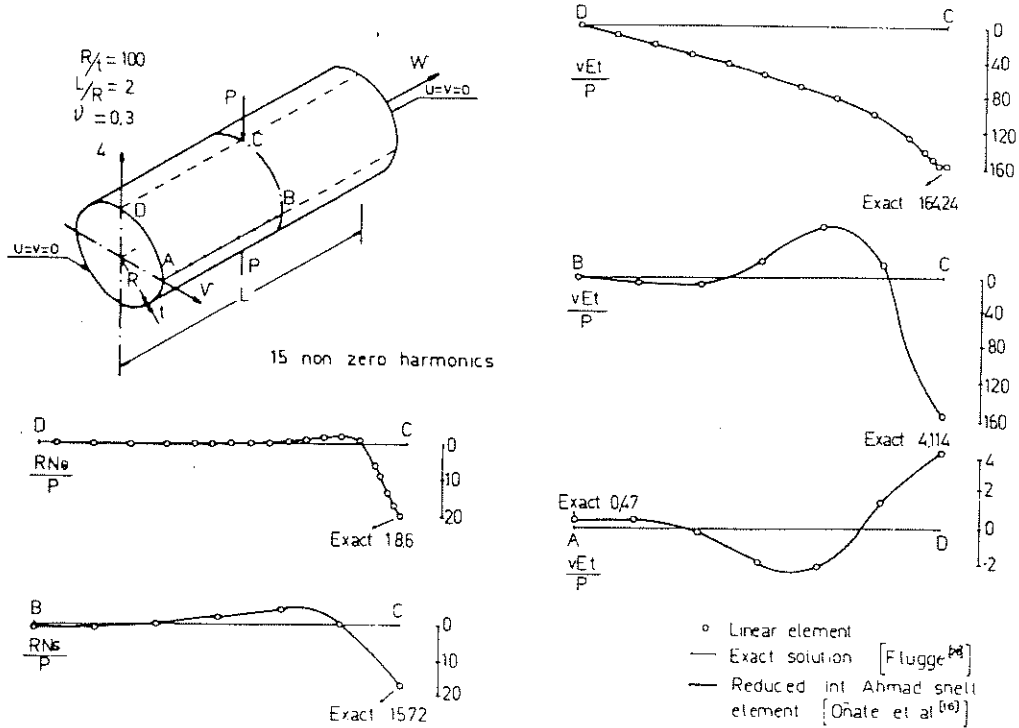


Fig. 12. Pinched cylindrical shell. Displacements and axial forces along several sections.

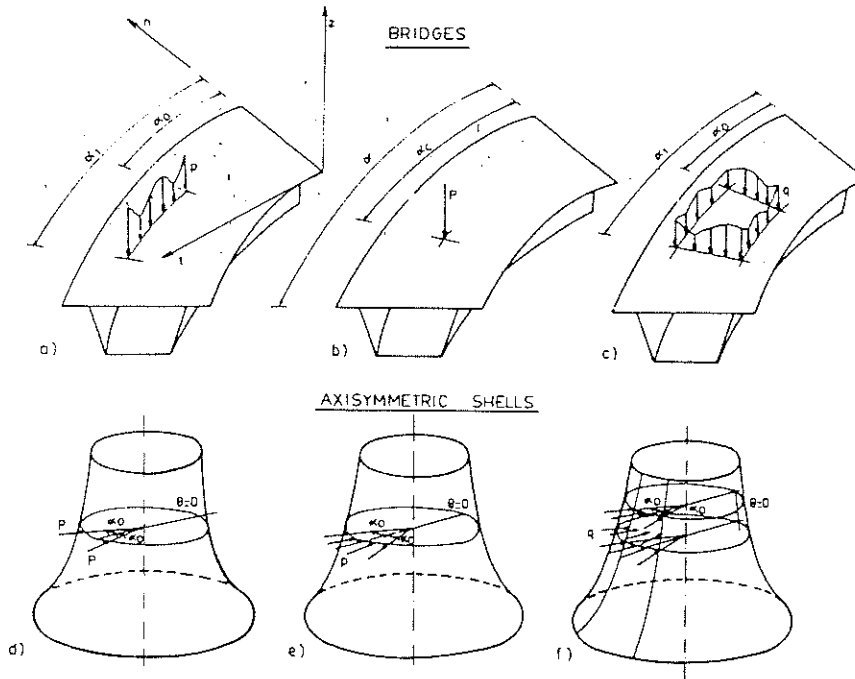


Fig. 13. Different types of loading for bridges and axisymmetric shells.

section can be treated in a simple and unified form using Mindlin's strip displacement formulation. Moreover, the problem is extremely simplified if two noded linear strip elements with a single quadrature integrating point are used. The element, thus formulated, can deal successfully with thick and thin bridges, plates and axisymmetric shells. The unified character of the general formulation allows to implement very easily all the computational aspects in a single computer program which, thus, can deal with a wide variety of practical engineering prob-

lems. The one-dimensional nature of the analysis makes the formulation specially suitable for its implementation in deck computers. Current lines of research in this area are the extension of the general formulation to deal with skew plates and bridges, intermediate diaphragms and continuous supports. The formulation is also suited for the development of a unified approach for the dynamic analysis of plate, bridge and axisymmetric shell structures. Extreme care, however, must be taken when dealing with axisymmetric shells since the reduced integrating

linear element presents a propagating zero energy mode in this case. This problem has been the recent subject of interest of research and alternative mixed formulations which seem to overcome this difficulty have already been suggested [29]. However, the displacement formulation here proposed can indeed produce directly very good results for these problems if higher order quadratic, cubic, or hierarchical strip elements are used. Details about this subject will be presented in a near future.

REFERENCES

1. Y. K. Cheung, Finite strip method analysis of elastic slabs. *Proc. Am. Soc. Civ. Engrg* 94, 1365-1378 (1968).
2. Y. K. Cheung, The finite strip method in the analysis of elastic plates with two opposite simple supported ends. *Proc. Instit. Civ. Engrs* 40, 1-7 (1968).
3. Y. K. Cheung, Analysis of box girder bridges by finite strip method. *Am. Concr. Ins. Publications*, SP 26, 357-378 (1969).
4. Y. K. Cheung, Folded plate structures by finite strip-method. *Am. Soc. Civ. Engrs* 96, 2963-2979 (1969).
5. Y. K. Cheung, The analysis of cylindrical orthotropic curved bridge decks. *Pub. Int. Ass. Struct. Engrg* 29, 41-52 (1969).
6. Y. K. Cheung, *The Finite Strip Method in Structural Analysis*, p. 232. Pergamon Press, Oxford (1976).
7. Y. C. Loo and Y. A. R. Cusens, A refined finite strip method for the analysis of orthotropic plates. *Proc. Instit. Civ. Engrs* 48, 85-91 (1970).
8. Y. C. Loo and Y. A. R. Cusens, The finite strip method in bridge engineering. *Viewpoint* 220 (1978).
9. K. J. Willam and A. C. Scordelis, Analysis of orthotropic folded plates with eccentric stiffeners. Report No. SESM 70-2. Dept. of Civil Engrg, Univ. of California, Berkeley (1970).
10. R. D. Mindlin, Influence of rotatory inertia and shear on flexural motion of isotropic elastic plates. *J. Appl. Mech.* 18, 31-38 (1951).
11. P. R. Benson and E. Hinton, A thick finite strip solution for static, free vibration and stability problems. *Int. J. Num. Meth. Engrg* 10, 665-678 (1976).
12. E. Oñate, Comparisons of finite strip methods for the analysis of box girder bridges. Msc. Thesis, Civ. Engr. Dep., Univ. Col. of Swansea (1976).
13. E. D. L. Pugh, E. Hinton and Y. O. C. Zienkiewicz, A study of quadrilateral plate bending elements with reduced integration. *Int. J. Num. Meth. Engrg* 12, 1059-1079 (1978).
14. T. J. R. Hughes, M. Cohen and Y. M. Haroun, Reduced and selective integration techniques in the finite element analysis of plates. *Nucl. Engrg Design* 46, 203-222 (1978).
15. T. J. R. Hughes and Y. M. Cohen, The heterosis finite element for plate bending. *Comp. Structures* 9, 445-450 (1978).
16. E. Oñate, E. Hinton and Y. N. Glover, Techniques for improving the performance of Ahmad shell elements. *Int. Conf. Appl. Num. Modelling*. Edited by Pentech Press, Madrid (1979).

17. B. Suarez, La formulación de Bandas finitas de Reissner Mindlin para análisis de placas, puentes y láminas de revolución. Ph.D. Thesis, E.T.S. Ing. Caminos, Barcelona (1982).
18. E. Oñate and B. Suarez, A comparison of the linear quadratic and cubic Mindlin strip elements for the analysis of thick and thin plates. *Comput. Structures* 17, 427-439 (1983).
19. K. Washizu, *Variational Methods in Elasticity and Plasticity*. Pergamon Press, Oxford (1975).
20. O. C. Zienkiewicz, O. C. Bauer, J. Morgan and K. Y. E. Oñate, A simple and efficient element for axisymmetric shells. *Int. J. Num. Meth. Engrs* 11, 1545-1558 (1977).
21. A. Coull and Y. P. C. Das, Analysis of curved bridge decks. *Proc. Instit. Civ. Engrs* 37, 75-85 (1967).
22. J. Thorpe, Ph.D. Thesis, University of Dundee (1976).
23. F. Sawko and Y. P. A. Merriman, An annular segment finite element for plate bending. *Int. J. Num. Meth. Engrs* 3, 119-129 (1971).
24. A. Fam and Y. C. Turkstra, A finite element method for box bridge analysis. *Comput. Structures* 5, 179-186 (1975).
25. E. Oñate, Comparación entre las formulaciones de la banda finite para análisis de puentes. Monografía. Inst. Ed. Torroga, No. 362, Madrid (1980).
26. W. Flugge, *Stresses in Shells*, p. 525. Springer-Verlag, Berlin (1973).
27. G. M. Lindberg, M. D. Olson and Y. G. R. Cowper, New developments in the finite element analysis of shells. *Struc. Material Laboratory*, p. 1-38 (1969).
28. S. Ahmad, B. M. Irons and Y. O. C. Zienkiewicz, Curved thick shell and membrane elements with particular reference to axisymmetric problems. *Proc. 2nd Conf. Matrix Methods in Struct. Mech.*, Wright-Patterson, A. F. Base, Ohio (1968).
29. R. Ohajon and B. Nicolas-Vullierme, An efficient shell finite element for the computation of the vibrations of fluid structure systems of revolution. *Presented to the SMIRT 6*, Paris, pp. 17-21, August 1981.
30. J. Vykutil, Explicit stiffness matrix of multipurpose linear element. *Int. J. Num. Meth. Engrg* 17, 1877-1882 (1981).
31. O. C. Zienkiewicz, *The Finite Element Method*. McGraw-Hill, New York (1979).
32. S. Timoshenko and S. Woinowsky-Krieger, *Theory of Plates and Shells*, 2nd Edn. McGraw-Hill, New York (1959).

APPENDIX 1

Strain Matrix for the linear strip element

We will present here the explicit form of the linear strip strain matrix $[\hat{B}^{*i}]^e$ which it relates the local strip generalized strains with the global displacements for the i th harmonic term.

For a linear two noded strip we have

$$[\hat{B}^{*i}]^e = [\hat{B}_1^{*i}, \hat{B}_2^{*i}]^e$$

where $[\hat{B}_i^{*i}]^e$ can be written in the following general form for the different structures studied in this paper:

$$\hat{B}_i^{*i} = \begin{bmatrix} \frac{(-1)^i S}{a^e} & 0 & \frac{(-1)^i C}{a^e} & 0 & 0 & 0 \\ \frac{1}{2F^e} & -\frac{A}{2F^e} & 0 & 0 & 0 & 0 \\ \frac{AS}{2F^e} & \left(\frac{(-1)^i S}{a^e} - \frac{S}{2F^e}\right) & \frac{AC}{2F^e} & 0 & 0 & 0 \\ 0 & 0 & 0 & \frac{(-1)^i}{a^e} & 0 & 0 \\ 0 & 0 & 0 & \frac{S}{2F^e} & -\frac{AS}{2F^e} & \frac{AC}{2F^e} \\ 0 & -\frac{(-1)^i C}{a^e F^e} & 0 & \frac{A}{2F^e} & \left(\frac{(-1)^i}{a^e} - \frac{S}{2F^e}\right) S & -\left(\frac{(-1)^i}{a^e} - \frac{S}{2F^e}\right) C \\ -\frac{(-1)^i C}{a^e} & 0 & \frac{(-1)^i S}{a^e} & \frac{1}{2} & 0 & 0 \\ -\frac{AC}{2F^e} & \frac{C}{2F^e} & \frac{AS}{2F^e} & 0 & \frac{S}{2} & -\frac{C}{2} \end{bmatrix} \quad (A1)$$

where for

Curved bridges

- $S = \sin \phi$
- $C = \cos \phi$, where ϕ is the strip orientation angle (see Fig. 3)
- $A = l\pi/\alpha$, where α is the angle of the bridge (see Fig. 3)
- a^e = width of the strip e
- \bar{r}^e = radius of the center of the strip e .

Straight bridges

It coincides exactly with eqn (A1) making

- (1) $A/\bar{r}^e = \hat{A} = l\pi/b$ with b the length of the bridge (see Fig. 1).
- (2) $\bar{r}^e = \infty$ in the rest of the terms.

Axisymmetric shells

Identical to eqn (A1) with $A = -l$

Plates

For curved plates the $5 \times 3 [\hat{\mathbf{B}}_i^*]^e$ matrix contains the terms inside the dotted line in eqn (A1).
For straight plates the same matrix applies making $A/\bar{r}^e = l\pi/b$ and $\bar{r}^e = \infty$ in the rest of the terms.

APPENDIX 2

Loading vectors for the linear strip

(a) *Curved and straight bridges*

(1) *Line load acting along the bridge longitudinal direction at node i (Fig. 13a).*

$$\mathbf{f}_i^l = \frac{r_i \alpha}{l\pi} [P_u \hat{C}, P_v \hat{S}, P_w \hat{C}, P_{\theta_1} \hat{C}, P_{\theta_2} \hat{S}, 0]^T \quad (A2)$$

where

$$\begin{aligned} \hat{C} &= \cos \frac{l\pi}{\alpha} \alpha_0 - \cos \frac{l\pi}{\alpha} \alpha_1 \\ \hat{S} &= \sin \frac{l\pi}{\alpha} \alpha_1 - \sin \frac{l\pi}{\alpha} \alpha_0. \end{aligned} \quad (A3)$$

For straight bridges $r_i \alpha = b$; $l\pi/\alpha = l\pi/b$; $\alpha_0 = b_0$ and $\alpha_1 = b_1$.

(2) *Point load acting at $\theta = \alpha_c$ at node i (Fig. 13b).*

$$\mathbf{f}_i^l = [P_u \bar{S}, P_u \bar{C}, P_w \bar{S}, P_{\theta_2} \bar{S}, P_{\theta_1} \bar{C}, 0]^T \quad (A4)$$

where

$$\bar{S} = \sin \frac{l\pi \alpha_c}{\alpha} \text{ and } \bar{C} = \cos \frac{l\pi \alpha_c}{\alpha}. \quad (A5)$$

For straight bridges $l\pi \alpha_c/\alpha = l\pi b_c/b$.

(3) *Uniformly distributed loading acting in element e (Fig. 13c)*

$$[\mathbf{f}_i^l]^e = \frac{\alpha^e \bar{r}^e a^e}{2\pi l} [t_u \hat{C}, t_v \hat{S}, t_w \hat{C}, t_{\theta_1} \hat{C}, t_{\theta_2} \hat{S}, 0]^T$$

\hat{C} and \hat{S} like in eqn (A3). a^e and \bar{r}^e are respectively the width and radius of the strip evaluated at the strip mid point. For straight bridges $\bar{r}^e \alpha = b$ and $l\pi/\alpha = l\pi/b$.

(4) *Self weight.*

$$[\mathbf{f}_i^l]^e = \frac{\rho^e g \alpha^e \bar{r}^e a^e \bar{r}^e}{2l\pi} (1 - (-1)^{2p}) [0, 0, -1, 0, 0, 0]^T$$

where ρ^e and t^e are the density and element thickness respectively. \bar{r}_e and a^e like in (3) and g is the gravity acceleration.

For straight bridges $\alpha \bar{r}^e = b$.

(b) *Axisymmetric shells: Symmetric loading*

(1) *Line load along a circumference (see Fig. 13d) acting at node i.*

$$\mathbf{f}_i^0 = 2r_i \alpha_0 [P_u, 0, P_w, P_{\theta_2}, 0, 0]^T$$

$$\mathbf{f}_i^l = \frac{2r_i}{l} \sin l\alpha_0 \cos l\pi [P_u, 0, P_w, P_{\theta_2}, 0, 0]^T$$

(2) *Point load acting at node i (see Fig. 13e) at $\theta = \alpha_0$.*

$$\mathbf{f}_i^0 = 2[P_u, 0, P_w, P_{\theta_2}, 0, 0]^T$$

$$\mathbf{f}_i^l = 2 \cos l\pi \cos l\alpha_0 [P_u, 0, P_w, P_{\theta_2}, 0, 0]^T.$$

(3) *Uniformly distributed loading acting in elements (see Fig. 13f).*

$$\mathbf{f}_i^0 = \alpha_0 a^e \bar{r}^e [t_u, 0, t_w, t_{\theta_2}, 0]^T$$

$$\mathbf{f}_i^l = \frac{a^e \bar{r}^e}{l} \sin l\alpha_0 \cos l\pi [t_u, 0, t_w, t_{\theta_2}, 0]^T.$$

Self weight

$$\mathbf{f}_i^0 = a^e \pi \bar{r}^e \rho^e g^e [0, 0, -1, 0, 0, 0]^T$$

$$\mathbf{f}_i^l = 0.$$